第 35 卷第 10 期
2019 年 10 月

无 机 化 学 学 报
CHINESE JOURNAL OF INORGANIC CHEMISTRY

Vol.35 No.10
1821-1833

大柴旦富硼浓缩盐卤中硼酸镁盐稀释结晶动力学

彭姣玉[1,2] 张 波[1,2] 陈 婧[1,2,3] 董亚萍*[,1,2] 李 武[1,4]

([1]中国科学院青海盐湖研究所,中国科学院盐湖资源综合高效利用重点实验室,西宁 810008)

([2]青海省盐湖资源综合利用工程技术中心,西宁 810008)

([3]中国科学院大学,北京 100049)

([4]青海省盐湖资源化学重点实验室,西宁 810008)

摘要:采用动力学法研究了富硼浓缩盐卤稀释过程硼酸镁盐的结晶动力学,重点探讨了温度、稀释比和硼浓度对结晶过程的影响。利用单纯形优化法配合 Runge-Kutta 微分方程组数值解法对实验数据进行拟合,给出了结晶动力学方程和结晶速率。结果表明,低温、高硼浓度和中间稀释比有利于硼酸镁盐的结晶析出,最优条件下析硼率(以 B_2O_3 计)高达 88%;结晶速率随硼浓度的增加和温度的降低快速增大;反应级数表明稀释结晶过程硼酸镁盐结晶主要受多核表面反应控制,同时提出了结晶相转化机理。

关键词:含硼盐卤;稀释;结晶动力学;硼酸镁盐

中图分类号:O643.1;O614.22;P578.93 **文献标识码**:A **文章编号**:1001-4861(2019)10-1821-13

DOI:10.11862/CJIC.2019.209

Crystallization Kinetics of Mg-Borates Precipitating from Diluted Boron-Containing Brine of Da Qaidam Saline Lake

PENG Jiao-Yu[1,2] ZHANG Bo[1,2] CHEN Jing[1,2,3] DONG Ya-Ping*[,1,2] LI Wu[1,4]

([1]*Key Laboratory of Comprehensive and Highly Efficient Utilization of Salt Lake Resources, Qinghai Institute of Salt Lakes, Chinese Academy of Sciences, Xining* 810008, *China*)

([2]*Qinghai Engineering and Technology Research Center of Comprehensive Utilization of Salt Lake Resources, Xining* 810008, *China*)

([3]*University of Chinese Academy of Sciences, Beijing* 100049, *China*)

([4]*Key Laboratory of Salt Lake Resources Chemistry of Qinghai Province, Xining* 810008, *China*)

Abstract: The crystallization kinetics of Mg-borates from different diluted brines was investigated by dynamical method. With the aid of simple optimum method and Runge-Kutta digital solution of differential equations, the experimental data was fitted by computer and the optimum kinetic equations of Mg-borates were obtained. Factors such as temperature, mass dilution ratios and boron concentrations during crystallization were tested. The crystallization rate was also calculated based on the kinetic equations. The results show that low temperature, high boron concentration and medium dilution ratio favor the Mg-borates crystallization. The boron yield would be more than 88% in B_2O_3 under the optimized condition. The kinetic parameters indicate that almost all of the crystallization mechanisms of Mg-borates in diluted brine are polynuclear layer controlled growth. Besides, the crystallization reactions in diluted solutions were also proposed.

Keywords: boron-containing brine; dilution; crystallization kinetics; Mg-borates

收稿日期:2019-01-23。收修改稿日期:2019-07-30。

国家青年科学基金(No.21501187),中国科学院西部之光人才培养项目(No.Y710091015)和盐湖化工联合基金面上项目(No.U1607103)资助。

*通信联系人。E-mail:Dongyaping@hotmail.com

0 Introduction

The new process of "crystallization by dilution" was firstly reported by Gao et al.[1-2] during study on the chemistry of borate in sulfate-type salt lake of Da Qaidam, in China. It refers to that borates could be accumulated in the concentrated brine throughout solar evaporation process, and keep stable at room temperature for a few months and do not crystallize until reach to the maximum solubility (5.82% in the form of B_2O_3)[3], while diluting this boron-concentrated brine with water can accelerate the precipitation of Mg-borates from aqueous solutions. Different hydrated Mg-borates, such as inderite (kurnakovite), hungchaoite, and macallisterite, can be crystallized out after dilution for a period of time, not only from brines with different dilution ratios for the same time period, but also from the same diluted brine after setting different periods[1,4-6]. This phenomenon explained the forming and mineralization of borate minerals deposited on Da Qaidam salt lake bottom [7-9], especially for the minerogenetic mechanism of pinnoite [10-12]. Furthermore, since the boron content in Mg-borate precipitates was more than 35% in the form of B_2O_3, which is much higher than boron ores (5%~30% B_2O_3) in China[13]. The high grade Mg-borate salts could be used as raw materials for industrial production of boron compound. Therefore, the "crystallization by dilution" would provide an economical method for the boron extraction from brine. However, since the magnesium borates have a high supersolubility and need a long time to achieve the solid-liquid equilibrium, which often causes a slow crystallization rate and low boron recovery during dilution process, it is of great importance to study the crystallization kinetics of Mg-borates from diluted brines. The objective of the present study was to investigate the crystallization kinetics and transformation mechanism of Mg-borates from different diluted brines by dynamical method. Factors such as temperature, dilution ratio and boron concentration on the Mg-borates crystallization were studied. The results obtained would provide fundamental data and theories for the efficient separation of boron resource from brine using dilution method.

1 Dynamic model

Gao et al.[14-19] had studied the crystallization kinetics of Mg-borates from MgO-$n$$B_2O_3$-$MgCl_2$/$MgSO_4$-$H_2O$ supersaturated solutions. In their studies, an appropriate mathematical modification of Nielsen′s polynuclear layer and mononuclear layer controlled growth mechanism[20-21] has been made, and the kinetic crystallization reaction equations of Mg-borates in supersaturated solutions are given as follows:

MA model: $-\mathrm{d}c/\mathrm{d}t=k_1(c_0-c)^{2/3}(c_0-c_\infty)^p$

MB model: $-\mathrm{d}c/\mathrm{d}t=k_2(c_0-c)^{4/3}(c_0-c_\infty)^p$

where MA and MB models correspond to the polynuclear layer and mononuclear layer controlled growth mechanism, respectively; k_1 and k_2 are the rate constants, c_0 and c_∞ are the initial concentration and equilibrium concentration of boron in solution, respectively; p is the reaction order referring to 1, 2, 3, and 4. Thus, four kinetic equations such as MA-1 (MB-1), MA-2 (MB-2), MA-3 (MB-3) and MA-4(MB-4) are obtained. Generally, the crystallization mechanism controlled by MB model needs higher reaction energy and longer inducing period compared with the MA model.

Based on the simple optimum method and Runge-Kutta digital solution of differential equations[14], the experimental data of c-t curve was fitted and the optimum kinetic equation of Mg-borates was calculated by computer, as shown in Fig.1. The c_0 value is considered as the boron concentration at the point of initial precipitation of solid phase, the $c_{\infty,0}$ is the initial value of equilibrium concentration of boron estimated less than the last value of experimental data. Because Mg-borates often have a high supersolubility and require a long period of time (more than half a year) to establish the solid-liquid equilibrium, it is difficult to determine the c_∞ value experimentally. The k_0 is also the initial value of the rate constant. The relative error E_r was defined as: $E_r=(c_{c,i}-c_{e,i})/c_{e,i}\times 100\%$. $c_{c,i}$ and $c_{e,i}$ are the calculation data and experimental data at t_i time period, respectively. The precision used was 10^{-7}. Among all the obtained MA and

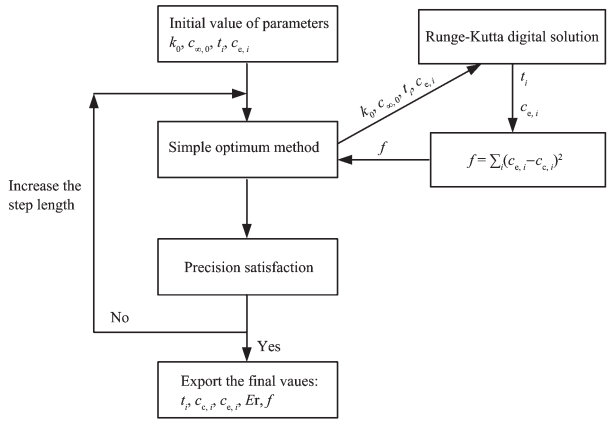

Fig.1　Schematic diagram of calculation procedure

MB kinetic equations, the suitable equation is selected when the values of E_r are no more than 5.0%.

In the present study, the boron-concentrated brine system can be referred as $MgO\text{-}2B_2O_3\text{-}MgSO_4\text{-}MgCl_2\text{-}H_2O$, which is similar to that of Gao′s studies. Therefore, we choose the MA and MB models to calculate the kinetic equations of Mg-borates precipitated from different diluted brines.

2　Experimental

2.1　Materials

A boron-containing brine (1.28% B_2O_3), saturated with bischofite ($MgCl_2\cdot6H_2O$), was obtained from Da Qaidam salt lake and concentrated further by evaporation at (298.15±3) K after the addition of $Na_2SO_4\cdot10H_2O$ solid. The concentration of boron in concentrated brines was 2.60%, 3.78% and 4.96% in the form of B_2O_3 (Table 1). The $Na_2SO_4\cdot10H_2O$ solid was recrystallized from mirabilite ores. Deionized water (resistivity, 18.25 MΩ·cm) was used in all experiments.

Table 1　Compositions of the brine used in experiments

Brine	Density / ($g\cdot cm^{-3}$)	pH	Mass fraction of ion / %						
			Na^+	Mg^{2+}	K^+	B^{3+} (B_2O_3)	Cl^-	SO_4^{2-}	Li^+
Da Qaidam (L0)	1.362 2	4.39	0.107	8.86	0.048	1.28	24.47	2.29	0.144
Brine L1	1.348 1	4.50	−0.051	8.70	0.056	2.60	22.90	3.23	0.246
Brine L2	1.394 5	4.43	0.016	8.80	0.063	3.78	23.22	2.91	0.301
Brine L3	—	4.31	0.055	8.71	0.078	4.96	22.32	3.42	0.353

2.2　Measurement of crystallization kinetics

The crystallization experiments were performed as follows[1]: an amount of the boron-concentrated brine was diluted with some water. The diluted brine was placed in a well-sealed glass vessel at constant temperature and stirred *ca.* 5 min each day to promote the precipitation of solid phase. When the solid phase began to precipitate from the diluted brine, some solution samples were taken out using a porous filter (Pore size: 3~4 μm) for boron concentration analysis. The sampling experiments were carried out every one or three days until the solution concentration of boron changed little or remained basically constant. Then the mixtures were filtered, and the resultant sediment was washed using some water and absolute alcohol, respectively, and dried in a vacuum drying oven for 24 h. The obtained solid phases were characterized by X-ray diffraction (XRD, PRO PANalytical X′Pert, Cu $K\alpha_1$, λ=0.154 nm) with a tube voltage and current of 40 kV and 30 mA, respectively. The powder pattern was measured in a scanning range from 5° to 70°. The composition of solid was analyzed by titration.

During the crystallization process, the boron concentrations used were 2.60%, 3.78% and 4.96% in the form of B_2O_3, and the mass dilution ratios (m_{water}/m_{brine}) tested were 0.50, 1.0 and 2.0. The temperature used was 258.15, 277.15 and 298.15 K. The experiments at low temperature (258.15 and 277.15 K) were achieved by placing in a refrigerator and that of 298.15 K was settled in water bath.

2.3　Chemical analysis

The titration analysis of brine and solid compositions was based on a previous publication[22]. The Mg^{2+} ion was analyzed by complexometric titration with ethylene diamine tetraacetic acid (EDTA). The K^+ ion was analyzed by quaternary ammonium back

titration. The Li^+ ion was determined by the flame atomic absorption spectrophotometer (AAS, AAnalyst 800, PE of USA). The Cl^- ion and boron was analyzed by mercurimetry and mannitol conversion acid base titration, respectively. The SO_4^{2-} ion was analyzed by the gravimetric method. While the Na^+ ion concentration in brine was calculated using the ion charge balance principle. The accuracy of these analyses was ±0.1%~±0.3%.

3 Results and discussion

3.1 Solid phase analysis

The XRD patterns of precipitates crystallized from diluted brines are shown in Fig.2. And the solid phase composition is listed in Table 2. The water content in precipitates was obtained by subtracting the mass of MgO and B_2O_3 from the total mass. As shown in Table 2, at 1.0 dilution ratio, when boron concentration was less than 3.78% in B_2O_3, the only triborates such as magnesium borate hydroxide ($MgB_3O_3(OH)_5\cdot 6H_2O$) and inderite ($MgB_3O_3(OH)_5\cdot 5H_2O$) had crystallized out from the diluted brines. As the boron concentration increased to 4.96% B_2O_3, the tetraborate of hungchaoite ($MgB_4O_5(OH)_4\cdot 7H_2O$) appeared in the precipitates at temperature lower than 277.15 K. This is because the high boron concentration and low temperature favored the formation of $[B_4O_5(OH)_4]^{2-}$ ion by polymerization. Besides, the content of B_2O_3 in precipitates varied in a range of 35%~40%, much higher than the grade ($w_{B_2O_3}\geqslant 12\%$) requested for chemical processing of borate minerals in China.

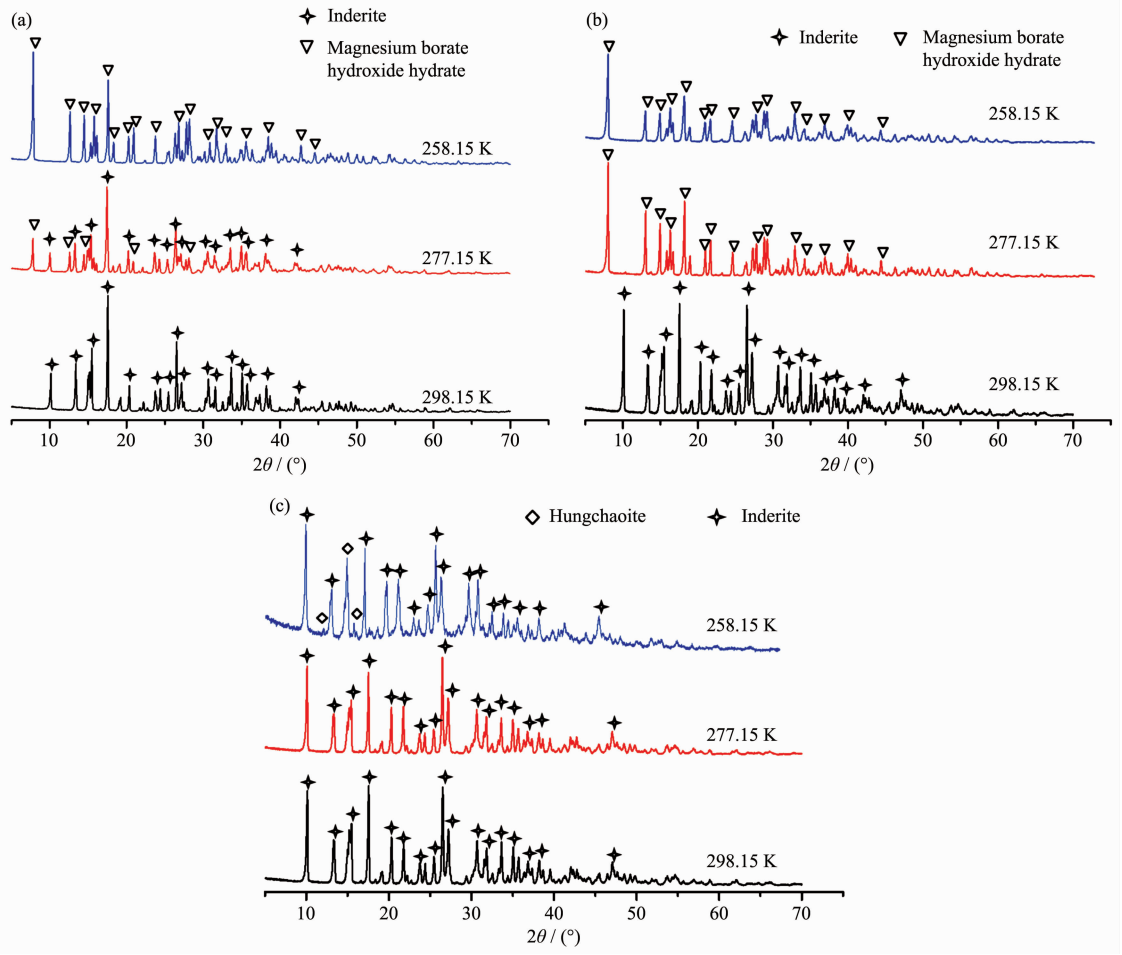

Dilution ratio=1.0

Fig.2 XRD patterns of solid phases crystallized from diluted brines with various boron concentrations: (a) 2.60%; (b) 3.78%; (c) 4.96%

Table 2　Analyses of solid phases crystallized from diluted brines

c_{boron} / % (*w*/*w*)	Dilution ratio	*T* / ℃	w_{MgO} / % (*w*/*w*)	$w_{B_2O_3}$ / % (*w*/*w*)	w_{H_2O} / % (*w*/*w*)	n_{MgO}:$n_{B_2O_3}$:n_{H_2O}	Solid phase determined by XRD	Formula
2.60	1.0	298.15	14.38	37.80	47.82	1.00:1.52:7.44	Magnesium borate hydroxide hydrate	$2MgO·3B_2O_3·15H_2O$
	1.0	277.15	14.05	36.91	49.04	1.00:1.52:7.81	Inderite+Magnesium borate hydroxide hydrate	$2MgO·3B_2O_3·15H_2O$+ $2MgO·3B_2O_3·17H_2O$
	1.0	258.15	13.57	35.10	51.34	1.00:1.50:8.47	Magnesium borate hydroxide hydrate	$2MgO·3B_2O_3·17H_2O$
3.78	1.0	298.15	14.40	37.94	47.66	1.00:1.53:7.41	Inderite	$2MgO·3B_2O_3·15H_2O$
	1.0	277.15	13.62	35.52	50.86	1.00:1.51:8.36	Magnesium borate hydroxide hydrate	$2MgO·3B_2O_3·17H_2O$
	1.0	258.15	13.55	35.16	51.30	1.00:1.50:8.47	Magnesium borate hydroxide hydrate	$2MgO·3B_2O_3·17H_2O$
4.96	1.0	298.15	14.37	37.99	47.65	1.00:1.53:7.42	Inderite	$2MgO·3B_2O_3·15H_2O$
	1.0	277.15	12.73	40.06	47.21	1.00:1.82:8.29	Inderite+Hungchaoite	$2MgO·3B_2O_3·15H_2O$+ $MgO·2B_2O_3·9H_2O$
	1.0	258.15	12.50	38.34	49.17	1.00:1.78:8.80	Inderite+Hungchaoite	$2MgO·3B_2O_3·15H_2O$+ $MgO·2B_2O_3·9H_2O$

3.2　Effects of temperature on crystallization

Fig.3 shows the effect of temperature on the crystallization process ($c_{B_2O_3}$-*t* curve) of Mg-borates from 2.60% and 4.96% boron (B_2O_3) brines at 1.0 dilution ratio, respectively.

As shown in Fig.3, the crystallization process appeared in the shape of reversed S curve including inducing period, crystallization and phase equilibrium stages. The time of inducing period decreased with the increasing of temperature and boron concentrations. While the total time period, throughout the crystallization process, shortened greatly with the decreasing of temperature and an increasing in boron concentrations due to higher supersaturation. For instance, the crystallization time shortened twice (from 1 400 to 600 h) as boron(B_2O_3) concentration increased from 2.60% to 4.96% at 258.15 K. Besides, when the boron (B_2O_3) concentration increased to 4.96% (Fig.3b), It was noted that the crystallization time changed little at temperature less than 277.15 K. Because the boron (B_2O_3) concentration of 4.96% in brine is closed to the maximum supersolubility of Mg-borate (5.71%~5.81% B_2O_3)[3] in concentrated salt lake brine, the influence of boron concentration is predominant and further

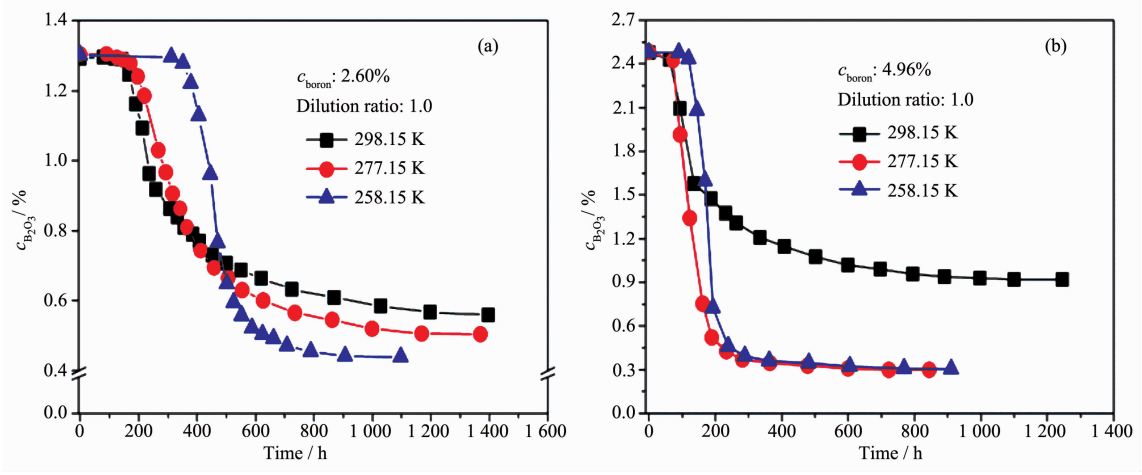

Fig.3　Effect of temperature on crystallization of Mg-borates

temperature reduction makes little effect on crystallization.

3.3 Effects of dilution ratio on crystallization

The influence of mass dilution ratio (m_{water}/m_{brine}) on the crystallization is shown in Fig.4. The boron (B_2O_3) concentration used was 2.60%. As can be seen, the phase equilibrium concentration of boron at dilution ratio of 0.50 was lower than that of 1.0 ratio at 258.15 K (Fig.4a). But the crystallization time of the former was twice longer than the latter due to the slower crystallization rate of Mg-borates at ratio of 0.50. At 277.15 K (Fig.4b), the crystallization time at ratio of 2.0 was shorter and the yield of boron was also lower compared with ratio of 1.0. According to our study, the diluted brine of 2.0 ratio would freeze when the temperature decreased from 277.15 to 258.15 K. Therefore, the dilution ratio ranging from 0.50 to 1.0 and the temperature below 277.15 K would be more preferable to the Mg-borates crystallization from salt lake brine.

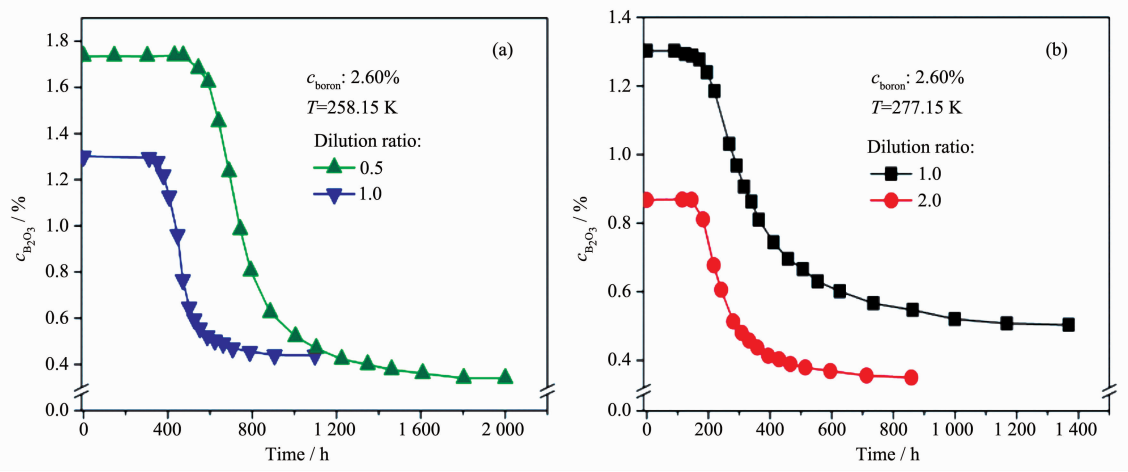

Fig.4 Effects of dilution ratio on crystallization of Mg-borates

3.4 Effects of boron concentration in brine on crystallization

As shown in Fig.5, the boron concentration affected dramatically on the yield of Mg-borates at ratio of 1.0, as well as the crystallization time. When boron (B_2O_3) concentration increased from 2.60% to 4.96%, the boron yield increased substantially from 61.4% to 88.0% in the form of B_2O_3. This result would offer considerable benefits to the boron extraction from salt lake brine by dilution method.

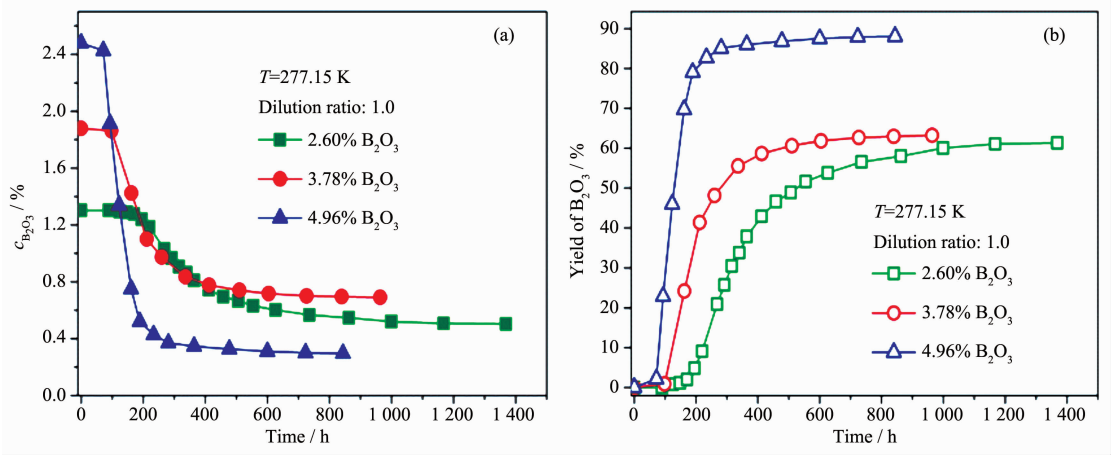

Fig.5 Effects of boron concentration in brine on crystallization of Mg-borates

3.5 Crystallization kinetics of Mg-borates

After calculations of the kinetic equation both from MA and MB models, the optimum kinetic equations of Mg-borates at 1.0 ratio with different temperature and boron concentrations were obtained as follows:

(1) 2.60% B_2O_3 boron-concentrated brine at 1.0 dilution ratio

298.15 K: $-dc/dt=0.0343\ 9(1.290-c)^{2/3}(c-0.540)^2$

277.15 K: $-dc/dt=0.0239\ 1(1.293-c)^{2/3}(c-0.490)^2$

258.15 K: $-dc/dt=0.0200\ 9(1.295-c)^{2/3}(c-0.440)$

(2) 3.78% B_2O_3 boron-concentrated brine at 1.0 dilution ratio

298.15 K: $-dc/dt=0.013\ 16(1.879-c)^{2/3}(c-0.650)^2$

277.15 K: $-dc/dt=0.025\ 46(1.863-c)^{2/3}(c-0.630)^2$

258.15 K: $-dc/dt=0.023\ 24(1.854-c)^{2/3}(c-0.570)^2$

(3) 4.96% B_2O_3 boron-concentrated brine at 1.0 dilution ratio

298.15 K: $-dc/dt=0.009\ 82(2.479-c)^{2/3}(c-0.850)^2$

277.15 K: $-dc/dt=0.013\ 73(2.427-c)^{2/3}(c-0.250)^2$

258.15 K: $-dc/dt=0.049\ 01(2.477-c)^{2/3}(c-0.220)^3$

The corresponding crystallization results of Mg-borates with boron (B_2O_3) concentration of 2.60%, 3.78% and 4.96% are shown in Table 3 to 5, respectively. The relative errors between the experimental and calculated data were plotted in Fig.6. As shown in Fig.6, most of the absolute values of relative error were less than 5% except for the minorities, suggesting the calculated data agreed well with the experiment one. According to the kinetic equations, it is known that the crystallization of Mg-borates is dominated by the polynuclear layer controlled growth mechanism. While the boron concentration increases to the maximum supersaturation level, the mononuclear layer controlled growth mechanism changes to be the predominant one at temperature of 258.15 K.

Fig.7 shows the crystallization rate ($-dc/dt$) of Mg-borates calculated by kinetic equations during crystallization. It is noted that the crystallization rate initially increases exponentially to a maximum value and then decreases dramatically with the crystallization time, particularly for the high boron concentration and low temperature. Furthermore, it is noticeable that the crystallization rate increases with the increasing of

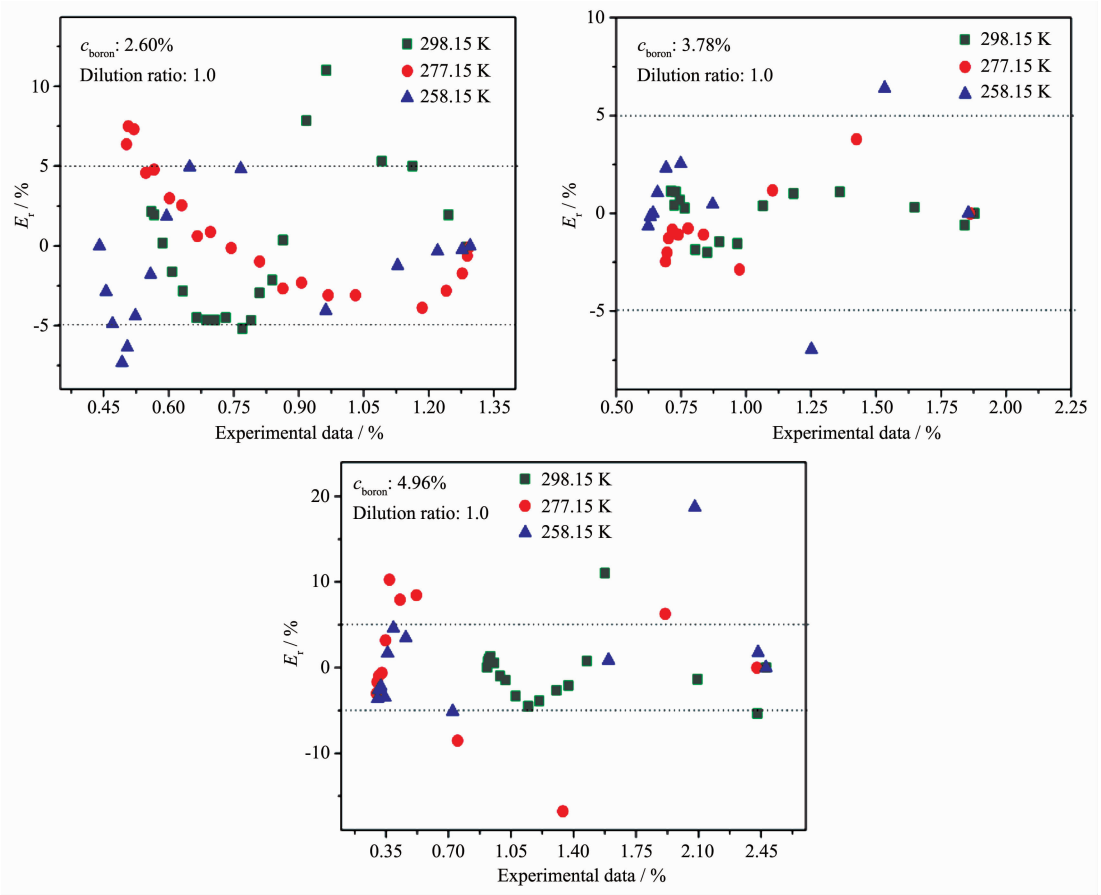

Fig.6　Concentrations of B_2O_3 and their errors between the experimental and calculated data during crystallization from diluted brine at ratio of 1.0

Table 3 Concentrations of B_2O_3 and their errors calculated by dynamic model during crystallization from 2.60% B_2O_3 diluted brine at ratio of 1.0*

298.15 K				277.15 K				258.15 K			
Time / h	c_e / %	c_c / %	E_r(MA-2) / %	Time / h	c_e / %	c_c / %	E_r(MA-2) / %	Time / h	c_e / %	c_c / %	E_r(MA-2) / %
0	1.292			0	1.303			0	1.302		
118.0	1.292			89.9	1.303			310.8	1.295	1.295	0.00
140.7	1.290	1.289	−0.08	125.1	1.293	1.292	−0.08	350.4	1.277	1.274	−0.23
166.7	1.246	1.270	1.93	148.2	1.289	1.281	−0.62	378.6	1.220	1.216	−0.33
190.5	1.163	1.221	4.99	170.9	1.277	1.255	−1.72	406.5	1.128	1.114	−1.24
213.3	1.092	1.150	5.31	195.5	1.240	1.205	−2.82	446.1	0.962	0.923	−4.05
235.8	0.964	1.070	11.00	220.2	1.185	1.139	−3.88	470.9	0.766	0.803	4.83
259.8	0.918	0.990	7.84	268.1	1.031	0.999	−3.10	501.3	0.648	0.680	4.94
307.6	0.864	0.867	0.35	291.9	0.968	0.938	−3.10	525.8	0.595	0.606	1.85
332.1	0.839	0.821	−2.15	315.8	0.906	0.885	−2.32	552.1	0.558	0.548	−1.79
355.8	0.810	0.786	−2.96	339.8	0.863	0.840	−2.67	587.5	0.523	0.500	−4.40
384.3	0.790	0.753	−4.68	363.9	0.810	0.802	−0.99	622.6	0.504	0.472	−6.35
408.5	0.770	0.730	−5.19	411.7	0.744	0.743	−0.13	662.1	0.492	0.456	−7.32
452.3	0.732	0.699	−4.51	458.8	0.696	0.702	0.86	707.4	0.470	0.447	−4.89
500.0	0.707	0.674	−4.67	506.8	0.666	0.670	0.60	788.8	0.455	0.442	−2.86
550.1	0.687	0.655	−4.66	554.8	0.630	0.646	2.54	906.4	0.440	0.440	0.00
620.0	0.665	0.635	−4.51	626.7	0.602	0.620	2.99	1 097.4	0.440	0.440	0.00
723.9	0.633	0.615	−2.84	735.4	0.566	0.593	4.77				
869.1	0.608	0.598	−1.64	862.7	0.547	0.572	4.57				
1 028.6	0.586	0.587	0.17	999.5	0.520	0.558	7.31				
1 197.3	0.567	0.578	1.94	1 167.9	0.507	0.545	7.50				
1 397.1	0.560	0.572	2.14	1 368.7	0.503	0.535	6.36				

*c_e: experimental data; c_c: calculated data

Table 4 Concentrations of B_2O_3 and their errors calculated by dynamic model during crystallization from 3.78% B_2O_3 diluted brine at ratio of 1.0*

298.15 K				277.15 K				258.15 K			
Time / h	c_e / %	c_c / %	E_r(MA-2) / %	Time / h	c_e / %	c_c / %	E_r(MA-2) / %	Time / h	c_e / %	c_c / %	E_r(MA-2) / %
0.00	1.879	1.879	0.00	0.00	1.880			0.00	1.874		
47.5	1.841	1.830	−0.60	98.3	1.863	1.863	0.00	95.6	1.868		
93.0	1.648	1.653	0.30	162.1	1.425	1.479	3.79	144.5	1.854	1.854	0.00
149.7	1.361	1.376	1.10	211.8	1.102	1.115	1.18	192.3	1.533	1.631	6.39
198.5	1.183	1.195	1.01	259.8	0.975	0.947	−2.87	245.2	1.251	1.164	−6.95
248.9	1.066	1.070	0.38	336.2	0.836	0.827	−1.08	321.4	0.871	0.875	0.46
325.1	0.968	0.953	−1.55	412.5	0.777	0.771	−0.77	396.5	0.748	0.767	2.54
400.2	0.898	0.885	−1.45	510.1	0.740	0.732	−1.08	484.1	0.692	0.708	2.31
487.2	0.851	0.834	−2.00	604.3	0.717	0.711	−0.84	604.4	0.659	0.666	1.06
607.2	0.806	0.791	−1.86	726.5	0.702	0.693	−1.28	735.0	0.642	0.642	0.00
710.3	0.765	0.767	0.26	839.7	0.696	0.682	−2.01	843.4	0.631	0.630	−0.16
809.1	0.746	0.751	0.67	963.6	0.691	0.674	−2.46	970.8	0.624	0.620	−0.64
906.2	0.730	0.738	1.10								
1 023.1	0.724	0.727	0.41								
1 116.0	0.712	0.720	1.12								

*c_e: experimental data; c_c: calculated data

Table 5 Concentrations of B_2O_3 and their errors calculated by dynamic model during crystallization from 4.96% B_2O_3 diluted brine at ratio of 1.0*

298.15 K				277.15 K				258.15 K			
Time / h	c_e / %	c_c / %	E_r(MA-2) / %	Time / h	c_e / %	c_c / %	E_r(MA-2) / %	Time / h	c_e / %	c_c / %	E_r(MA-2) / %
0.00	2.479	2.479	0.00	0.00	2.480			0.00	2.477		
61.6	2.430	2.299	−5.39	71.6	2.427	2.427	0.00	88.8	2.477	2.477	0.00
92.3	2.095	2.066	−1.38	93.4	1.913	2.033	6.27	118.7	2.433	2.476	1.77
134.8	1.577	1.751	11.03	122.9	1.340	1.115	−16.79	145.5	2.078	2.467	18.72
186.4	1.475	1.486	0.75	161.3	0.751	0.687	−8.52	169.3	1.595	1.609	0.88
230.4	1.373	1.344	−2.11	189.1	0.520	0.564	8.46	193.3	0.723	0.686	−5.12
263.3	1.305	1.270	−2.68	233.7	0.429	0.463	7.93	238.8	0.460	0.476	3.48
335.0	1.209	1.162	−3.89	281.0	0.370	0.408	10.27	288.3	0.391	0.409	4.60
407.2	1.147	1.095	−4.53	364.1	0.347	0.358	3.17	362.4	0.359	0.365	1.67
502.0	1.077	1.041	−3.34	477.7	0.327	0.325	−0.61	480.8	0.344	0.332	−3.49
598.8	1.020	1.005	−1.47	600.0	0.310	0.307	−0.97	604.2	0.321	0.314	−2.18
697.5	0.989	0.979	−1.01	723.0	0.300	0.295	−1.67	768.6	0.308	0.300	−2.60
794.0	0.956	0.961	0.52	843.5	0.297	0.288	−3.03	909.8	0.302	0.291	−3.64
889.5	0.936	0.948	1.28								
997.8	0.927	0.936	0.97								
1 100.6	0.921	0.927	0.65								
1 246.1	0.917	0.917	0.00								

*c_e: experimental data; c_c: calculated data

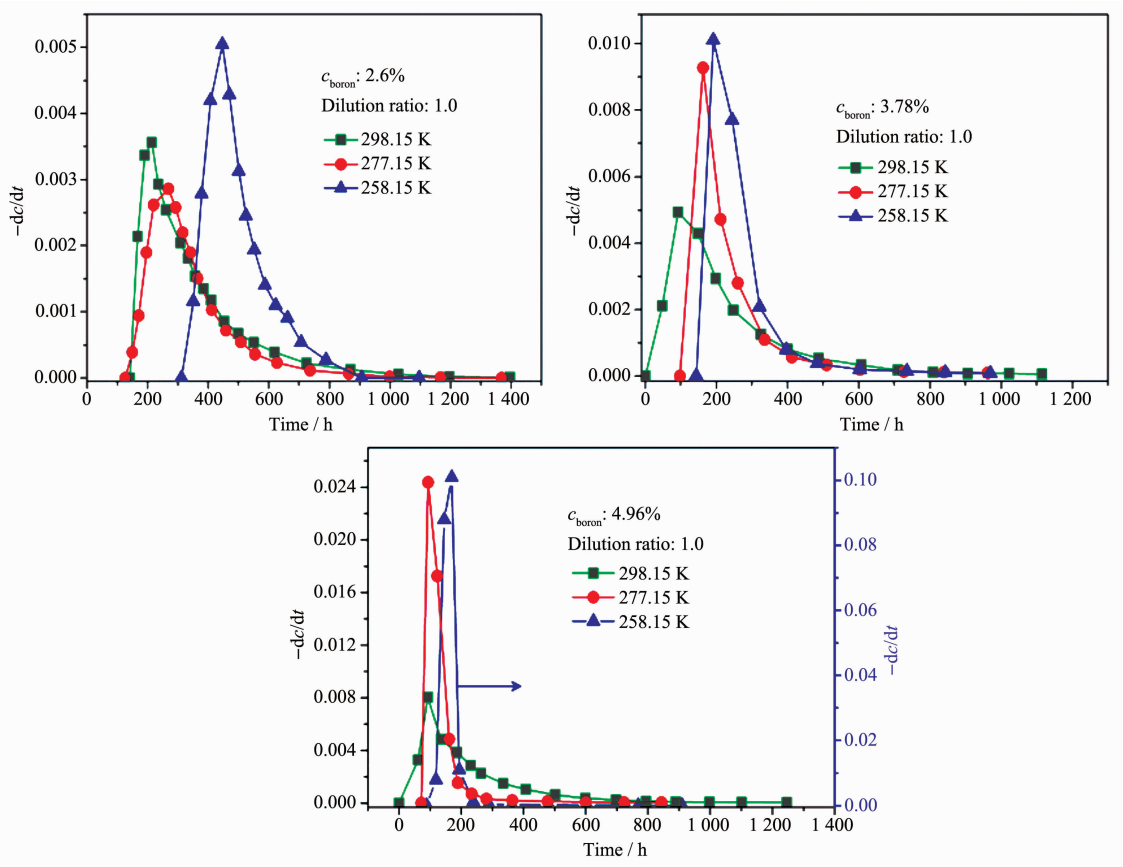

Fig.7　(−dc/dt)-t curves of solid phases crystallized from diluted brines with different boron concentrations and temperatures

boron concentrations and the drops of temperature, which explains the reason that the crystallization time of Mg-borates shortened dramatically with the rising in boron concentrations and also the lowering of temperature.

3.6　Transformation mechanism of Mg-borates

According to our earlier study[5,23], the Raman spectra of the diluted brine (c_{boron}=2.5%~4.7%) and the mother solution after precipitation were recorded at room temperature and it is found that the main boron forms in the diluted brine at ratio of 1.0 are $B(OH)_3$, $[B(OH)_4]^-$, and $[B_3O_3(OH)_4]^-$ anions. Species of $[B_5O_6(OH)_4]^-$ and $[B_4O_5(OH)_4]^{2-}$ ions are the minorities. But it changed after Mg-borates precipitation from the brine. The Raman intensity of the $[B_3O_3(OH)_4]^-$ ion decreased and the $[B(OH)_4]^-$, $[B_5O_6(OH)_4]^-$ and $[B_4O_5(OH)_4]^{2-}$ ions disappeared in the mother solution. This is because the $[B_3O_3(OH)_4]^-$ ion was used for Mg-borates precipitation and the boron concentration in solution decreased rapidly, which promotes the de-polymerization of $[B_5O_6(OH)_4]^-$ and $[B_4O_5(OH)_4]^{2-}$ in solution. Besides, the pH value of solution also decreased after precipitation and the solution became weak acidic. This reveals that the OH^- ion is also consumed for the Mg-borates precipitation. In this paper, since the boron concentration, dilution ratio, and the solid phases are similar to the earlier report, the phase transformations of inderite, magnesium borate hydroxide and hungchaoite happening in the diluted brine at ratio of 1.0 can be deduced as follows:

For the triborates, the trimers of $[B_3O_3(OH)_4]^-$ ion present in solution would couple a OH^- to form the $[B_3O_3(OH)_5]^{2-}$ ion and then react with $[Mg(H_2O)_6]^{2+}$ ion in solution to precipitate the triborates, the main reactions can be:

$$[B_3O_3(OH)_4]^- + OH^- \rightleftharpoons [B_3O_3(OH)_5]^- \quad (1)$$

$$Mg^{2+} + 6H_2O \rightleftharpoons [Mg(H_2O)_6]^{2+} \quad (2)$$

$$[B_3O_3(OH)_5]^{2-} + [Mg(H_2O)_6]^{2+} \rightleftharpoons MgB_3O_3(OH)_5 \cdot 5H_2O \downarrow + H_2O \quad (3)$$

(inderite)

$$[B_3O_3(OH)_5]^{2-}+[Mg(H_2O)_6]^{2+} \rightleftharpoons MgB_3O_3(OH)_5\cdot 6H_2O\downarrow \quad (4)$$

(magnesium borate hydroxide hydrate)

Among the reactions, since the $[B_3O_3(OH)_4]^-$ coupled a OH^- to form the $[B_3O_3(OH)_5]^{2-}$ ion, the solution pH value decreases after solid precipitation.

For the tetraborates, the lower temperature and increasing boron concentration favor the polymerizaiton of the $[B_3O_3(OH)_4]^-$ with $[B(OH)_4]^-$ to form the $[B_4O_5(OH)_4]^{2-}$ ion, and then $[B_4O_5(OH)_4]^{2-}$ react with $[Mg(H_2O)_6]^{2+}$ ion to precipitate the hungchaoite. The main reactions can be:

$$[B_3O_3(OH)_4]^-+OH^-+B(OH)_3 \rightleftharpoons [B_4O_5(OH)_4]^{2-}+2H_2O \quad (5)$$

$$Mg^{2+}+6H_2O \rightleftharpoons [Mg(H_2O)_6]^{2+} \quad (6)$$

$$[B_4O_5(OH)_4]^{2-}+[Mg(H_2O)_6]^{2+}+H_2O \rightleftharpoons MgB_4O_5(OH)_4\cdot 7H_2O\downarrow \quad (7)$$

(hungchaoite)

4 Conclusions

The boron-concentrated brine with system of $MgO\cdot 2B_2O_3$-$MgSO_4$-$MgCl_2$-H_2O was obtained by evaporation and the crystallization of Mg-borates from diluted brines was studied by the kinetic method. The major conclusions are as follows:

(1) The crystallization time, crystallization rate and boron yield are greatly influenced by temperature, dilution ratio and boron concentration. High boron concentration with medium dilution ratio and low temperature are found to be more beneficial to the boron crystallization and the boron yield obtained was more than 88% ($c_{B_2O_3}$), which is favorable to the boron extraction from salt lake brine by dilution method.

(2) According to the kinetic equations, the crystallization of Mg-borates in diluted brine is dominated by the mechanism of polynuclear layer controlled growth. However, as the boron concentration increases to the maximum supersaturation level and the temperature decreases to 258.15 K, the mononuclear layer controlled growth mechanism becomes the predominant one. Furthermore, the phase transformation mechanism of Mg-borates was also proposed based on the Raman spectra of borate ions in solution before or after precipitation.

The above results can provide useful information and technical support for the application of dilution method in boron separation from salt lake.

References:

[1] GAO Shi-Yang(高世扬), XU Kai-Feng(许开芬), LI Gang(李刚), et al. *Acta Chim. Sinica*(化学学报), **1986**,**44**:1229-1233

[2] GAO Shi-Yang(高世扬), FENG Jiu-Ning(冯九宁). *Chinese J. Inorg. Chem.*(无机化学学报), **1992**,**8**(1):68-70

[3] GAO Shi-Yang(高世扬), FU Ting-Jin(符廷进), WANG Jian-Zhong(王建中). *Chinese. J. Inorg. Chem.*(无机化学学报), **1985**,**1**:97-102

[4] Peng J Y, Bian S J, Zhang B, et al. *Hydrometallurgy*, **2017**, **174**:47-55

[5] PENG Jiao-Yu(彭姣玉). *Thesis for the Doctorate of University of Chinese Academy of Sciences*(中国科学院大学博士论文). **2016**.

[6] Peng J Y, Bian S J, Lin F, et al. *Phase Transitions*, **2017**,**90** (10):1025-1033

[7] GAO Chun-Liang(高春亮), YU Jun-Qing(余俊清), MIN Xiu-Yun(闵秀云), et al. *Journal of Salt Lake Research*(盐湖研究), **2015**,**23**(1):22-29

[8] GAO Chun-Liang(高春亮), YU Jun-Qing(余俊清), MIN Xiu-Yun(闵秀云), et al. *Acta Geol. Sin.*(地质学报), **2015**,**89**(3): 659-670

[9] GAO Shi-Yang(高世扬), LI Bing-Xiao(李秉孝). *Acta Mineralogica Sinica*(矿物学报), **1982**(2):107-112

[10]Lin F, Dong Y P, Peng J Y, et al. *Phase Transitions*, **2016**, **89**(6):558-567

[11]Peng J Y, Bian S J, Lin F, et al. *Phase Transitions*, **2017**,**90** (10):1025-1033

[12]LIU Zhi-Hong(刘志宏), HU Man-Cheng(胡满成), GAO Shi-Yang(高世扬), et al. *Geochimica*(地球化学), **2003**,**32**(6): 569-572

[13]ZHENG Xue-Jia(郑学家). *Production and Application of Boron Compounds*(硼化合物生产及应用). Beijing: Chemical Industry Press, **2008**:21-43

[14]GAO Shi-Yang(高世扬), CHEN Xue-An(陈学安), XIA Shu-Ping(夏树屏). *Acta Chim. Sinica*(化学学报), **1990**,**48**:1049-1056

[15]GAO Shi-Yang(高世扬), HUANG Fa-Qing(黄发清), XIA Shu-Ping(夏树屏). *Journal of Salt Lake Research*(盐湖研究), **1993**,**1**(1):38-48

[16]YAO Zhan-Li(姚占力), GAO Shi-Yang(高世扬), ZHU Li-

Xia(朱黎霞). *Chinese. J. Inorg. Chem.*(无机化学学报), **1995**,**11**(4):419-423

[17]ZHU Li-Xia(朱黎霞), GAO Shi-Yang(高世扬), XIA Shu-Ping(夏树屏), et al. *Chinese. J. Inorg. Chem.*(无机化学学报), **2000**,**16**(5):722-728

[18]MA Yu-Tao(马玉涛), XIA Shu-Ping(夏树屏), GAO Shi-Yang(高世扬). *Chemical Research and Application*(化学研究与应用), **2001**,**13**(6):636-640

[19]GAO Shi-Yang(高世扬), YAO Zhan-Li(姚占力), XIA Shu-Ping(夏树屏). *Acta Chim. Sinica*(化学学报), **1994**,**52**:10-22

[20]Nielsen A E. Acta Chem. Scand. 1959(13):784-802

[21]Nielsen A E. *Kinetics of Precipitation*. Oxford: Pergamon, **1964**.

[22]Analysis Room of Qinghai Institute of Salt Lakes, Chinese Academy of Sciences(中国科学院青海盐湖研究所分析室). *Workbook of Identication and Analysis Method of Salt Minerals*. 2*nd Ed.*(卤水和盐的分析方法.2 版). Beijing: Chemical Industry Press, **1988**.

[23]Peng J Y, Chen J, Dong Y P, et al. *Spectrochim. Acta Part A*, **2018**,**199**:367-375